Occurrence of a Bacterial Membrane Microdomain at the Cell Division Site Enriched in Phospholipids with Polyunsaturated Hydrocarbon Chains*[S]

Sho Sato[‡1], **Jun Kawamoto**[‡], **Satoshi B. Sato**[§], **Bunta Watanabe**[‡], **Jun Hiratake**[‡], **Nobuyoshi Esaki**[‡2], **and Tatsuo Kurihara**[‡3]

From the ‡Institute for Chemical Research, Kyoto University, Uji, Kyoto 611-0011 and the §Research Center for Low Temperature and Material Sciences, Kyoto University, Kyoto 606-8501, Japan

Background: Phospholipids containing polyunsaturated hydrocarbon chains play important roles in various biological membranes.

Results: Fluorescence microscopic analysis with a chemically synthesized fluorescent probe showed localization of phospholipids containing an eicosapentaenyl group at the bacterial cell division site.

Conclusion: Phospholipids containing polyunsaturated hydrocarbon chains form a membrane microdomain at the cell center, probably to promote cell division.

Significance: Hydrocarbon chain-dependent microdomain formation was visualized *in vivo*.

In this study, we found that phospholipids containing an eicosapentaenyl group form a novel membrane microdomain at the cell division site of a Gram-negative bacterium, *Shewanella livingstonensis* Ac10, using chemically synthesized fluorescent probes. The occurrence of membrane microdomains in eukaryotes and prokaryotes has been demonstrated with various imaging tools for phospholipids with different polar headgroups. However, few studies have focused on the hydrocarbon chain-dependent localization of membrane-resident phospholipids *in vivo*. We previously found that lack of eicosapentaenoic acid (EPA), a polyunsaturated fatty acid found at the *sn*-2 position of glycerophospholipids, causes a defect in cell division after DNA replication of *S. livingstonensis* Ac10. Here, we synthesized phospholipid probes labeled with a fluorescent 7-nitro-2,1,3-benzoxadiazol-4-yl (NBD) group to study the localization of EPA-containing phospholipids by fluorescence microscopy. A fluorescent probe in which EPA was bound to the glycerol backbone via an ester bond was found to be unsuitable for imaging because EPA was released from the probe by *in vivo* hydrolysis. To overcome this problem, we synthesized hydrolysis-resistant ether-type phospholipid probes. Using these probes, we found that the fluorescence localized between two nucleoids at the cell center during cell division when the cells were grown in the presence of the eicosapen-

taenyl group-containing probe (*N*-NBD-1-oleoyl-2-eicosapentaenyl-*sn*-glycero-3-phosphoethanolamine), whereas this localization was not observed with the oleyl group-containing control probe (*N*-NBD-1-oleoyl-2-oleyl-*sn*-glycero-3-phosphoethanolamine). Thus, phospholipids containing an eicosapentaenyl group are specifically enriched at the cell division site. Formation of a membrane microdomain enriched in EPA-containing phospholipids at the nucleoid occlusion site probably facilitates cell division.

Biological membranes are composed of lipids and proteins and play essential roles in all living organisms in nutrient uptake, waste efflux, signal transduction, morphogenesis, etc. According to the fluid mosaic model proposed by Singer and Nicolson (1), it was previously assumed that lipids are homogeneously distributed in biological membranes. However, this view was considerably modified by the discovery of membrane microdomains, each of which is supposed to have specific physiological functions.

Various lipid molecules form membrane microdomains in eukaryotes and prokaryotes. Eukaryotic cells contain membrane microdomains known as lipid rafts, which are enriched in sphingolipids and sterols (2). Lipid rafts serve as platforms for the colocalization of proteins involved in signaling and transport. In prokaryotes, cardiolipin microdomains exist at the poles and septa in the rod-shaped cells of *Escherichia coli*, *Bacillus subtilis*, and *Pseudomonas putida* (3, 4, 32). Recently, the membrane of *B. subtilis* was reported to contain microdomains functionally similar to the lipid rafts of eukaryotic cells (5). These observations indicate the importance of dissecting the distribution of individual lipid molecules in biological membranes to better understand the mechanisms behind biological phenomena observed at the cell membrane.

Bacterial Membrane Microdomain at the Cell Division Site

The long-chain ω-3 polyunsaturated fatty acids eicosapentaenoic acid (EPA[4]; 5,8,11,14,17-all-*cis*-20:5) and docosahexaenoic acid (DHA, 4,7,10,13,16,19-all-*cis*-22:6) have been attracting a great deal of attention mainly because of their beneficial effects on human health (6–8). EPA and DHA occur in the membranes of various organisms, including mammals and bacteria, as acyl chains of phospholipids. EPA and DHA serve as precursors of various eicosanoids and autacoids (9). DHA interacts with membrane-associated G protein-coupled receptors to support their function (10–12). In EPA-producing bacteria, EPA plays a beneficial role in cell division (13, 14). However, the molecular mechanisms of EPA and DHA action are not well defined, in particular, their roles in coordinating the spatial organization of the phospholipids that contain them in biological membranes.

The Gram-negative bacterium *Shewanella livingstonensis* Ac10, which produces EPA as an *sn*-2-acyl chain of phosphatidylethanolamine (PE) and phosphatidylglycerol (PG) (13, 15), is an excellent model organism for studies on *in vivo* EPA function for the following reasons (13, 15–17). (i) The genes coding for EPA synthase are known, enabling the construction of an EPA-less mutant by disruption of these genes. (ii) The phenotype of the EPA-less mutant is clear; depletion of EPA causes growth retardation at low temperatures and produces filamentous cells because of a defect in cell division. (iii) The structure-function relationship of EPA can be studied by externally adding a series of EPA analogs to the culture medium. (iv) The whole genome sequence is available for this bacterium. (v) The methods for the genetic manipulation of this bacterium have been established. (vi) As a bacterium, it has a much simpler membrane system than eukaryotic cells.

To gain more insight into the function of the EPA-containing phospholipids in the cell membrane, we synthesized fluorescent molecular probes in this study to visualize the distribution of phospholipids containing polyunsaturated hydrocarbon chains. Advances have recently been made in the methods for labeling small molecules to visualize their subcellular localization. For phospholipids, methods have been reported for visualization of phosphatidylserine (18), PE (19), phosphatidylcholine (20, 21), phosphatidic acid (22), and sphingomyelin (21, 23). However, hydrocarbon chain-dependent localization of phospholipids cannot be visualized using the currently available molecular probes. To achieve this, we introduced a fluorescent group into the headgroup of phospholipids. A polyunsaturated hydrocarbon chain was bound to the phospholipids via an ether bond. (An ester bond did not work because it was hydrolyzed in *S. livingstonensis* Ac10, resulting in the release of the polyunsaturated hydrocarbon chain from the probe molecule.) Using this fluorescent probe, we found that phospholipids with an eicosapentaenyl group are enriched at the cell division site of *S. livingstonensis* Ac10. This is in accordance with the physiological function of EPA-containing phospholipids in the cell division of this bacterium. These results greatly contribute to understanding the *in vivo* function of polyunsaturated fatty acids and indicate the usefulness of the probe we synthesized.

EXPERIMENTAL PROCEDURES

Synthesis of Fluorescent Phospholipid Probes—The 7-nitro-2,1,3-benzoxadiazol-4-yl (NBD)-labeled phospholipids shown in Fig. 1 were chemically synthesized as described under supplemental "Experimental Procedures."

Bacterial Strain and Growth Conditions—The EPA-less mutant of *S. livingstonensis* Ac10 used in this study was constructed by the disruption of *orf5*, one of the genes required for EPA synthesis (13). We previously found that this EPA-less mutant is longer than the wild-type strain because of retardation of cell division after DNA replication; this longer bacterial length facilitates microscopic analysis of the phospholipid subcellular localization, as fluorescence microscopic analysis of the much shorter wild-type strain cells is difficult. The cells were grown in LB medium containing 50 μg/ml rifampicin and 40 μg/ml kanamycin for 48 h at 18 °C. The seed culture was used to inoculate 5 ml of LB medium containing the various NBD-labeled phospholipids (0.13 mM) chemically synthesized in this study. The phospholipid solution in chloroform was dried in a sterilized tube with nitrogen gas, resolubilized in 80 μl of ethanol, and then hydrated with 5 ml of LB medium to a final concentration of 0.13 mM by vortexing. The cells were cultured at 6 °C for 250 h until they reached stationary phase.

Fluorescence Microscopic Analysis—The culture (100 μl each) was sampled at 150, 200, and 250 h, and the fluorescence images were obtained using an epifluorescence microscope. For nuclear labeling, the cells collected at 250 h were treated with Hoechst 33342 (final concentration of 25 μg/ml) and washed twice with 200 μl of buffer containing 0.75 M sucrose and 10 mM Tris-HCl (pH 7.5). The fluorescence images were also obtained after dithionite treatment of the cells to quench the NBD fluorescence in the outer leaflet of the outer membrane. Further details are described under supplemental "Experimental Procedures."

Electrospray Ionization (ESI) MS Analysis of Phospholipids—After fluorescence microscopic analysis, lipids were extracted from the residual sample by the Bligh and Dyer method (24) and analyzed by ESI-MS. The details of the ESI-MS analysis are described under supplemental "Experimental Procedures."

Dithionite Assay for Measuring Lipid Distribution in Inner (IM) and Outer (OM) Membranes—To determine the distribution of NBD-labeled phospholipids in the IM and OM of the bacterium, we employed a fluorescence-quenching assay using sodium dithionite. For this assay, the following three samples were prepared: non-treated, lysozyme-treated, and lysozyme- and Triton X-100-treated cells (supplemental Fig. S1*A*). In the non-treated samples, only NBD-labeled phospholipids at the outer leaflet of the OM (OM_{out}) were accessible by dithionite, and their fluorescence was quenched. In the lysozyme-treated samples, the OM was disrupted, and both the inner leaflet of the OM (OM_{in}) and the outer leaflet of the IM (IM_{out}), in addition to the OM_{out}, became accessible to dithionite for fluorescence quenching. In the lysozyme- and Triton X-100-treated sam-

---

[4] The abbreviations used are: EPA, eicosapentaenoic acid; DHA, docosahexaenoic acid; PE, phosphatidylethanolamine; PG, phosphatidylglycerol; NBD, 7-nitro-2,1,3-benzoxadiazol-4-yl; ESI, electrospray ionization; IM, inner membrane; OM, outer membrane; OM_{out}, OM outer leaflet; OM_{in}, OM inner leaflet; IM_{out}, IM outer leaflet; IM_{in}, IM inner leaflet; OLA, oleic acid.
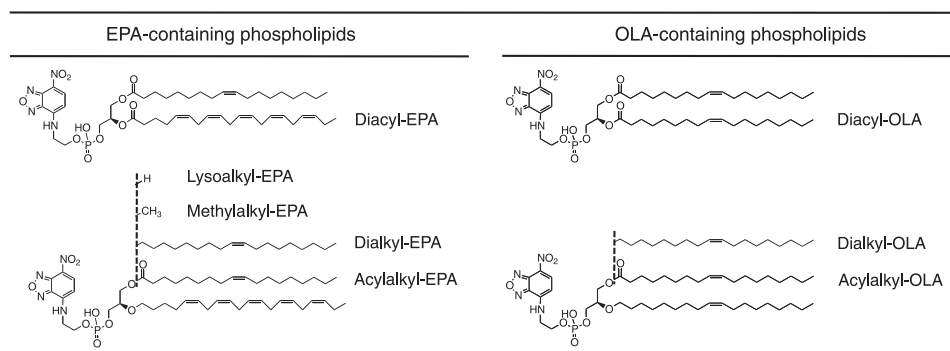
FIGURE 1. **NBD-labeled phospholipids synthesized in this study.** Diacyl-EPA, diacyl-OLA, acylalkyl-EPA, acylalkyl-OLA, dialkyl-EPA, and dialkyl-OLA were named after the binding mode between the glycerol moiety and the hydrocarbon chains, as well as the hydrocarbon chain species at the *sn*-2 position. Acylalkyl-EPA, acylalkyl-OLA, dialkyl-EPA, dialkyl-OLA, methylalkyl-EPA, and lysoalkyl-EPA correspond to compounds **34**, **33**, **14**, **21**, **38**, and **40**, respectively, in supplemental Scheme S1.

ples, both the OM and IM were disrupted, and the inner leaflet of the IM (IM_{in}), as well as the OM_{out}, OM_{in}, and IM_{out}, became accessible to dithionite. Further details of the dithionite assay are described under supplemental "Experimental Procedures."

RESULTS

Fate of Fluorescence-labeled Diacyl Phospholipids in Cell Membranes—To visualize EPA-containing phospholipids in *S. livingstonensis* Ac10, we first synthesized a fluorescence-labeled phospholipid, *N*-NBD-1-oleoyl-2-eicosapentaenoyl-*sn*-glycero-3-phosphoethanolamine (diacyl-EPA) (Fig. 1; see supplemental "Experimental Procedures" for the synthesis). EPA was introduced into the *sn*-2 position because a polyunsaturated fatty acid is primarily found at this position in phospholipids in *S. livingstonensis* Ac10 and other organisms (25). The fluorescent NBD group was introduced into the headgroup to avoid modification of the hydrocarbon chain, which was characterized in this study. As a control, we synthesized *N*-NBD-1,2-dioleoyl-*sn*-glycero-3-phosphoethanolamine (diacyl-oleic acid (OLA)), which contained the oleoyl group instead of the eicosapentaenoyl group at the *sn*-2 position (Fig. 1; see supplemental "Experimental Procedures" for the synthesis). In these phospholipids, OLA (9-*cis*-18:1) was introduced into the *sn*-1 position because OLA and OLA-containing phospholipids were shown to have neutral effects on the phenotype of the EPA-less mutant (13, 15).

S. livingstonensis Ac10 was grown at 6 °C in LB medium supplemented with diacyl-EPA or diacyl-OLA, and the cellular phospholipids were analyzed by ESI-MS. We found that the amounts of diacyl-EPA and diacyl-OLA in cellular membranes gradually decreased during cultivation for 166 h, whereas PEs and PGs containing EPA or OLA gradually increased (supplemental Fig. S2). The results suggest that diacyl-EPA and diacyl-OLA are hydrolyzed to yield free fatty acids, which are then incorporated into cellular PEs and PGs. The OM phospholipase A likely catalyzed this hydrolysis (15, 26, 27). The NBD moiety of diacyl-EPA and diacyl-OLA was not introduced into cellular phospholipids as evaluated by ESI-MS analysis. In accordance with the ESI-MS data, fluorescence microscopic analysis revealed that the diacyl-EPA and diacyl-OLA fluorescence was hardly detected at 150 h and thereafter (Fig. 2). Thus, we learned that although EPA and OLA could be incorporated into

PE and PG, they could not be tracked visually because the fluorescent NBD moiety was hydrolyzed and lost. Therefore, the NBD-labeled diacyl phospholipids were not suitable for continual visualization of EPA-containing phospholipids *in vivo*.

Synthesis of Fluorescent Eicosapentaenyl Group-containing Phospholipids—For continual visualization of phospholipids *in vivo*, we synthesized NBD-containing hydrolysis-resistant PE derivatives to prevent the release of the hydrocarbon chain from the phospholipids. It was expected that replacement of the ester bond at the *sn*-2 position of phospholipids with an ether bond would suppress the hydrolytic release of the hydrocarbon chain from the glycerol backbone. Accordingly, we synthesized the following ether phospholipids to use in the *in vivo* imaging experiments: *N*-NBD-1-oleoyl-2-eicosapentaenyl-*sn*-glycero-3-phosphoethanolamine (acylalkyl-EPA), *N*-NBD-1-oleoyl-2-oleyl-*sn*-glycero-3-phosphoethanolamine (acylalkyl-OLA), *N*-NBD-1-oleoyl-2-eicosapentaenyl-*sn*-glycero-3-phosphoethanolamine (dialkyl-EPA), and *N*-NBD-1,2-dioleyl-*sn*-glycero-3-phosphoethanolamine (dialkyl-OLA) (Fig. 1; see supplemental "Experimental Procedures" for the synthesis).

Cellular Uptake and Remodeling of Fluorescent Eicosapentaenyl Group-containing Phospholipids—We tested whether these synthetic ether phospholipids are incorporated into the cell membrane of *S. livingstonensis* Ac10. The total lipids isolated from the cells grown in the presence of acylalkyl-EPA, acylalkyl-OLA, dialkyl-EPA, or dialkyl-OLA were analyzed by ESI MS/MS (Figs. 3 and 4). NBD-labeled phospholipids were found in the cell membrane when any of the synthetic ether phospholipids were used (Fig. 3). We also found that acylalkyl-EPA and acylalkyl-OLA were hydrolyzed at the *sn*-1 (but not *sn*-2) position to yield *N*-NBD-2-eicosapentaenyl-*sn*-glycero-3-phosphoethanolamine (lysoalkyl-EPA) and *N*-NBD-2-oleyl-*sn*-glycero-3-phosphoethanolamine (lysoalkyl-OLA), respectively, during cultivation (Fig. 4, *white bars*). In addition to lysoalkyl-EPA and lysoalkyl-OLA, re-acylated NBD-labeled phospholipids containing two hydrocarbon chains were produced at 200 and 250 h (Fig. 4, *black bars*). The ratio of the total amount of the NBD-labeled phospholipids to the total amount of the unlabeled phospholipids in the cells grown in the presence of acylalkyl-EPA for 250 h was $9.8 \pm 3.1\%$. The composition of the fatty acyl chains at the *sn*-1 position of the NBD-
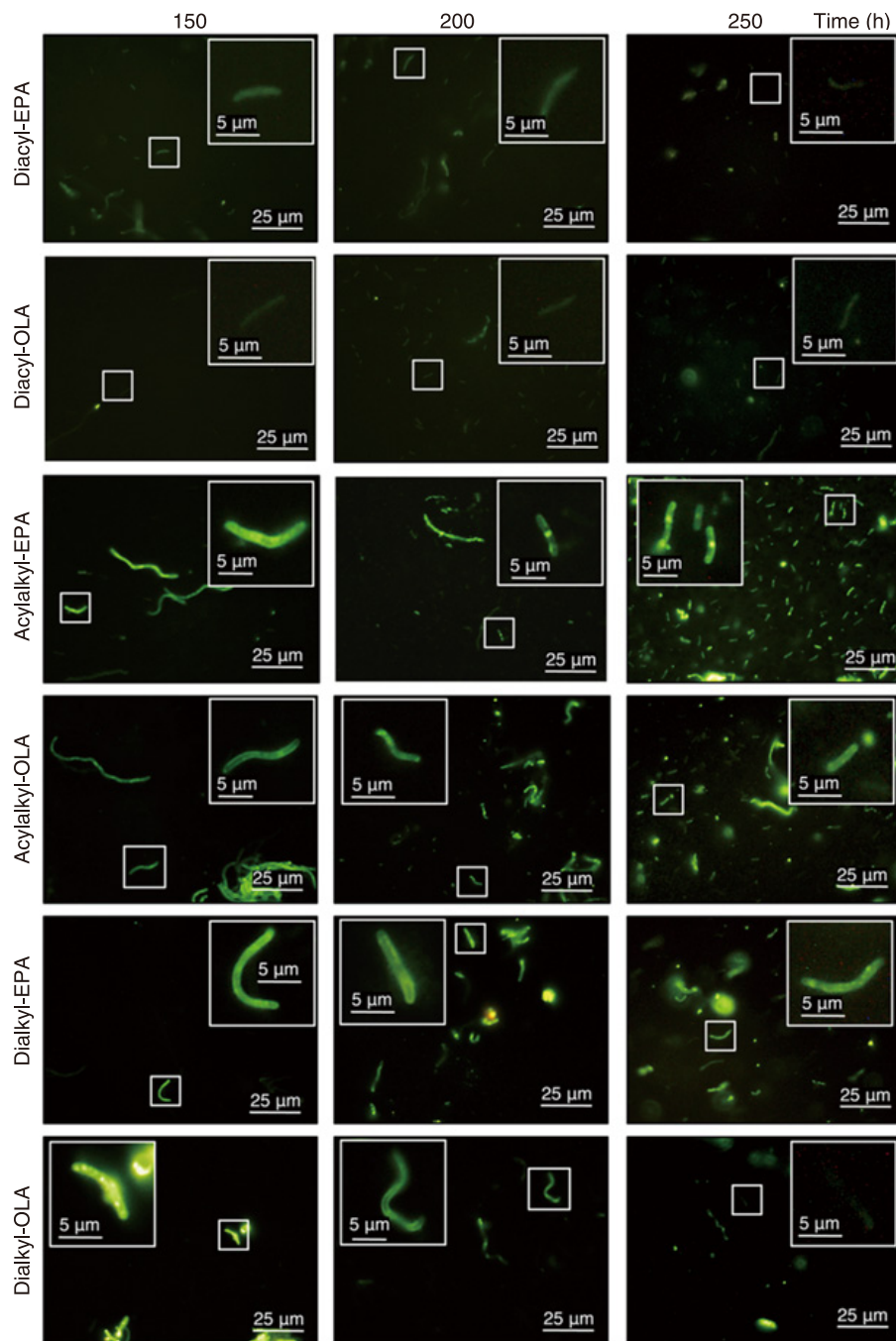
FIGURE 2. Fluorescence microscopic images of *S. livingstonensis* Ac10 grown in presence of NBD-labeled phospholipids (diacyl-EPA, diacyl-OLA, acylalkyl-EPA, acylalkyl-OLA, dialkyl-EPA, and dialkyl-OLA) for 150, 200, and 250 h.

labeled phospholipids derived from acylalkyl-EPA is shown in Table 1. These phospholipids, constituting 1–5% of the total NBD-labeled phospholipids, were produced by the incorporation of a bacterial fatty acyl chain into the *sn*-1 position. In contrast to acylalkyl-EPA and acylalkyl-OLA, dialkyl-EPA and dialkyl-OLA were incorporated into the cell membrane without remodeling because the ether bonds at the *sn*-1 and *sn*-2 positions are both resistant to hydrolysis (Fig. 4).

Distribution of NBD-labeled Phospholipids in IM and OM—S. livingstonensis Ac10 is a Gram-negative bacterium possessing both the OM and IM. We measured the amount of NBD-labeled phospholipids distributed in these membranes by the

dithionite quenching assay (see "Experimental Procedures" and supplemental "Experimental Procedures" for details). To identify the membrane-specific location of the NBD-labeled phospholipids, we prepared the following three samples from cells grown at 6 °C for 250 h: non-treated, lysozyme-treated, and lysozyme- and Triton X-100-treated cells (supplemental Fig. S1A). Using these samples, NBD-labeled phospholipids located in the OM_{out}, in the OM_{in} and IM_{out}, and in the IM_{in} can be measured. Note that the OM_{in} and IM_{out} cannot be distinguished by this assay.

We calculated the ratio of the NBD fluorescence at the OM_{out}, $OM_{in} + IM_{out}$, and IM_{in} in the cells grown in the pres-
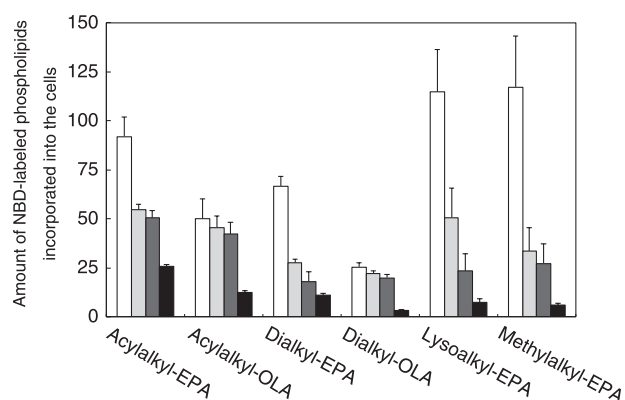
FIGURE 3. **Amount of NBD-labeled phospholipids incorporated into *S. livingstonensis* Ac10 cells grown in presence of acylalkyl-EPA, acylalkyl-OLA, dialkyl-EPA, dialkyl-OLA, lysoalkyl-EPA, and methylalkyl-EPA for 50 (*white bars*), 100 (*light gray bars*), 150 (*dark gray bars*), and 200 (*black bars*) h.** The amount was calculated as described under "Experimental Procedures" and supplemental "Experimental Procedures." The mean ± S.D. of three separate measurements is shown.
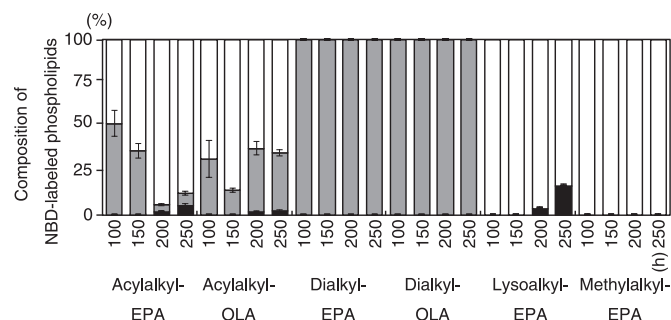

FIGURE 4. **Composition of NBD-labeled phospholipids in *S. livingstonensis* Ac10 cells.** The cells were grown in the presence of acylalkyl-EPA, acylalkyl-OLA, dialkyl-EPA, dialkyl-OLA, lysoalkyl-EPA, and methylalkyl-EPA for 100, 150, 200, and 250 h. The structures of NBD-labeled phospholipids extracted from the cells were analyzed by ESI-MS. *Gray bars*, externally added double-chain phospholipids; *white bars*, single-chain phospholipids derived from acylalkyl-EPA and acylalkyl-OLA and externally added lysoalkyl-EPA and methylalkyl-EPA; *black bars*, double-chain phospholipids produced in *S. livingstonensis* Ac10 by acylation at the *sn*-1 position of the single-chain phospholipids. The mean ± S.D. of three separate measurements is shown.

TABLE 1

Composition of the *sn*-1 acyl chain of NBD-labeled phospholipids from cells cultivated with acylalkyl-EPA and lysoalkyl-EPA

	Relative amount	
sn-1 Acyl chain	Acylalkyl-EPA	Lysoalkyl-EPA
	%	
13:0	4.0 ± 0.3	4.1 ± 0.6
13:1	1.2 ± 0.6	1.6 ± 0.6
14:0	4.0 ± 2.6	4.7 ± 2.6
14:1	1.6 ± 1.0	1.8 ± 1.0
15:0	19.0 ± 9.2	24.5 ± 12.3
15:1	0.9 ± 0.2	1.3 ± 0.6
16:0	0.7 ± 0.1	1.0 ± 0.2
16:1	29.6 ± 6.4	37.2 ± 11.4
17:0	6.6 ± 0.6	8.2 ± 0.7
17:1	3.3 ± 0.5	4.1 ± 0.2
18:0	2.1 ± 0.4	2.7 ± 0.6
18:1	27.0 ± 2.1	8.8 ± 1.1
20:5	ND[a]	ND

[a] ND, not determined.

ence of acylalkyl-EPA, acylalkyl-OLA, dialkyl-EPA, or dialkyl-OLA for 250 h (Fig. 5). For dialkyl-EPA and dialkyl-OLA, the NBD fluorescence was found at the OM_{out} and OM_{in} + OM_{out}, but almost no fluorescence was found at the IM_{in}. In contrast,
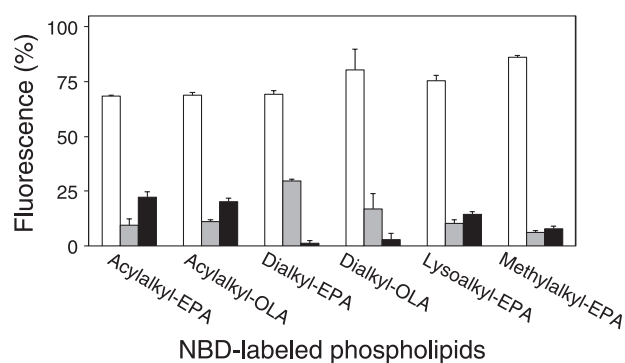

FIGURE 5. **Distribution of NBD-labeled phospholipids in OM_{out} (*white bars*), OM_{in} + IM_{out} (*gray bars*), and IM_{in} (*black bars*).** The cells were grown in the presence of the various NBD-labeled phospholipids indicated. The mean ± S.D. of three separate determinations is shown.

~25% of the fluorescence was found at the IM_{in} when acylalkyl-EPA or acylalkyl-OLA was added to the cells.

In these experiments, a large part of the NBD fluorescence was quenched even when non-treated cells were used. This was not due to quenching of NBD derivatives in the culture medium because the cells were washed well before dithionite treatment. The results rather indicate that a large part of the NBD-labeled phospholipids was localized in OM_{out}. This uneven distribution between the different membrane surfaces is probably due to slow flip-flop of the lipids.

Fluorescence Microscopic Analysis of Eicosapentaenyl Group-containing Phospholipids—We cultivated *S. livingstonensis* Ac10 at 6 °C in LB medium containing the NBD-labeled ether phospholipids (acylalkyl-EPA, acylalkyl-OLA, dialkyl-EPA, and dialkyl-OLA) for fluorescence microscopic analysis. These cells showed more intense fluorescence than those grown in the presence of diacyl-EPA or diacyl-OLA, except for the cells grown in the presence of dialkyl-OLA for 250 h (Fig. 2). The disappearance of the fluorescence from the cells grown in the presence of dialkyl-OLA was probably due to degradation of the NBD-labeled phospholipids or their elimination from the cells (Fig. 3). We found that the fluorescence was localized at the center of the cells when they were grown in the presence of acylalkyl-EPA for 200 h or longer, whereas this localization was not observed in cells grown in the presence of the acylalkyl-OLA control (Figs. 2 and 6). Fluorescence localization was also not observed in the dialkyl-EPA and dialkyl-OLA experiment (Fig. 2).

To further characterize the fluorescence localization, the cellular nucleoids were stained with Hoechst 33342 in cells grown with acylalkyl-EPA or acylalkyl-OLA for 250 h. Each of the 15 randomly chosen cells undergoing cell division was divided into seven equally sized sections, and the fluorescence intensities of NBD and Hoechst 33342 in each segment were measured (Fig. 6*B*). We found that the NBD-labeled ether phospholipids were localized at the nucleoid occlusion site at the center of the acylalkyl-EPA-treated cells undergoing cell division. This localization was not observed when acylalkyl-OLA was used. On the other hand, the same localization and cellular uptake and remodeling were observed when the *sn*-1-oleoyl group of acylalkyl-EPA was replaced with a palmitoleoyl group (data not shown). Thus, the fluorescence localization at the center of the
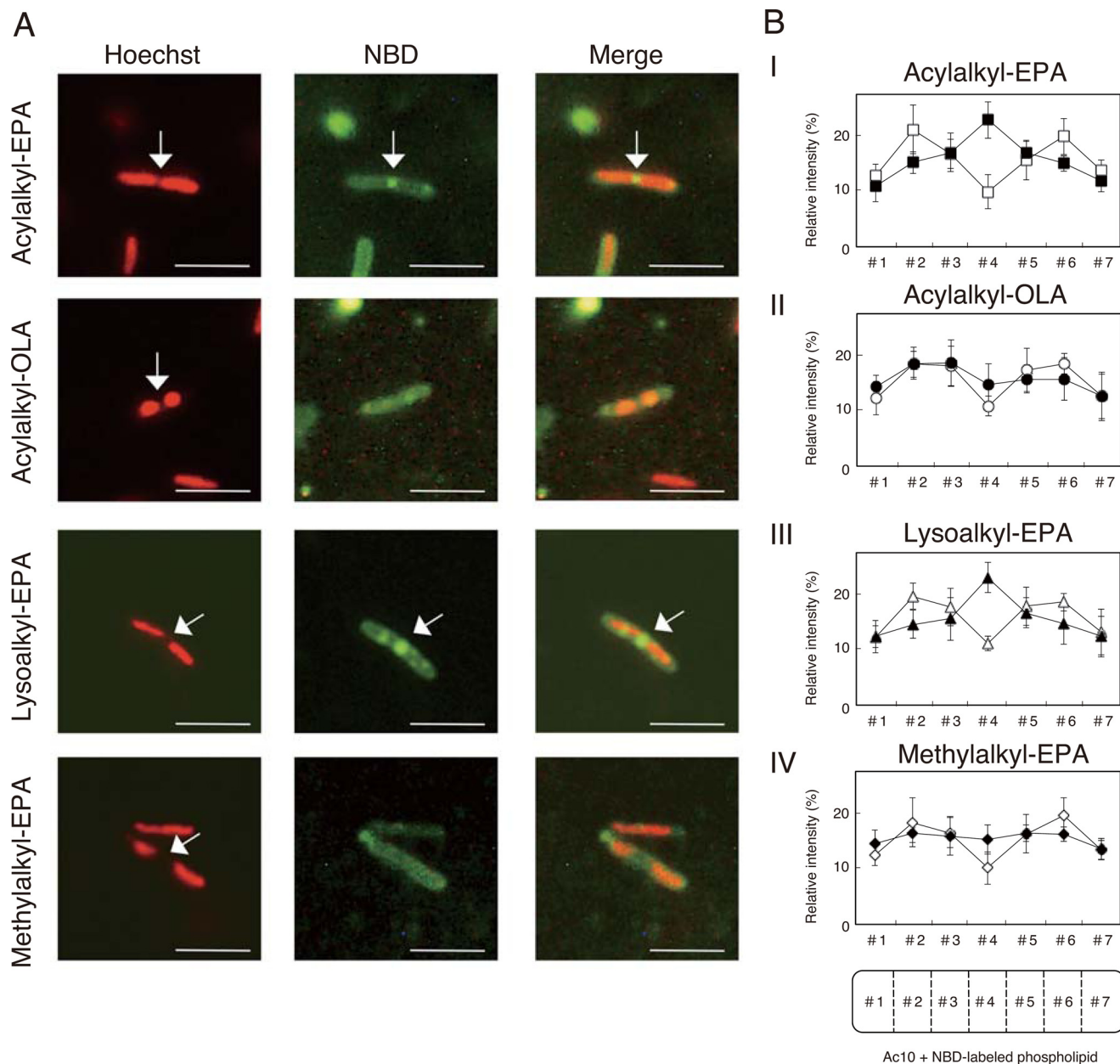
FIGURE 6. **Fluorescence microscopic images of *S. livingstonensis* Ac10 grown in presence of NBD-labeled phospholipids.** *A*, fluorescence microscopic images of the cells stained with Hoechst 33342 (false-colored red) (*left panels*) and NBD-labeled phospholipids (*center panels*) and merged images (*right panels*). The cells were grown at 6 °C for 250 h in the presence of the NBD-labeled phospholipids indicated on the left. *Scale bars* = 5 μm. *B*, quantification of subcellular localization of NBD-labeled phospholipids and acylalkyl-EPA (*panel I*), acylalkyl-OLA (*panel II*), lysoalkyl-EPA (*panel III*), and methylalkyl-EPA (*panel IV*) at 6 °C for 250 h. In each case, 15 cells during cell division were randomly chosen, and fluorescence intensities in seven equally sized sections of the cells (*#1–#7*) were determined using ImageJ software. *Closed symbols*, fluorescence of NBD-labeled phospholipids; *open symbols*, fluorescence of Hoechst 33342.

cells was dependent on the eicosapentaenyl group of the phospholipid. The localization we observed in these experiments is in accordance with the physiological importance of EPA-containing phospholipids in cell division.

Imaging of Lysoalkyl-EPA and Its Analog, N-NBD-1-methyl-2-eicosapentaenyl-sn-glycero-3-phosphoethanolamine (Methylalkyl-EPA), in Cell Membranes—As shown in Figs. 2 and 6, we found that NBD-labeled phospholipids were localized at the center of the cells when acylalkyl-EPA was added to the cells. Under this condition, some of the acylalkyl-EPA added to the cells was converted into lysoalkyl-EPA, which was subsequently re-acylated to form phospholipids with two hydrocarbon chains (Fig. 4). Thus, the fluorescent phospholipids localized at the center of the cells could be the acylalkyl-EPA added to the cells, the converted lysoalkyl-EPA, or the re-acylated phospholipids. To distinguish between these and to examine whether lysoalkyl-EPA produced from acylalkyl-EPA was localized at the center of the cells, we synthesized a lysoalkyl-EPA analog, methylalkyl-EPA, for *in vivo* imaging (Fig. 1; see supplemental "Experimental Procedures" for the synthesis). Methylalkyl-EPA retains the hydrophilicity of lysoalkyl-EPA, which is considered to be important for the molecule to traverse through the periplasmic space to reach the IM. However, unlike lysoalkyl-EPA, it is not susceptible to acy-
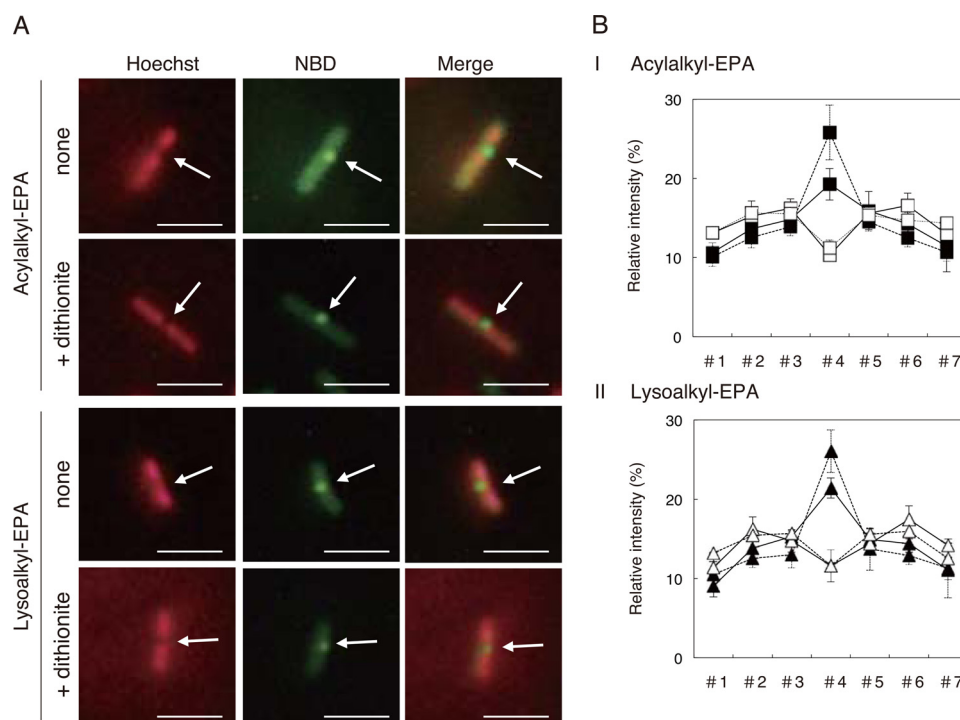
FIGURE 7. Fluorescence microscopic images of dithionite-treated *S. livingstonensis* Ac10 grown in presence of NBD-labeled phospholipids. *A*, fluorescence microscopic images of the cells stained with Hoechst 33342 (false-colored red) (*left panels*) and NBD-labeled phospholipids (*center panels*) and merged images (*right panels*). The cells were grown at 6 °C for 250 h in the presence of acylalkyl-EPA or lysoalkyl-EPA as indicated on the left. For each of the acylalkyl-EPA-labeled and lysoalkyl-EPA-labeled cells, fluorescence images with (*lower panels*) and without (*upper panels*) dithionite treatment are shown. *Scale bars* = 5 μm. *B*, quantification of the subcellular localization of NBD-labeled phospholipids and Hoechst 33342. The cells were grown in the presence of acylalkyl-EPA (*panel I*) and lysoalkyl-EPA (*panel II*) at 6 °C for 250 h. In each case, 15 cells during cell division were randomly chosen, and fluorescence intensities in seven equally sized sections of the cells (*#1–#7*) were determined using ImageJ software. *Closed symbols*, fluorescence of NBD-labeled phospholipids; *open symbols*, fluorescence of Hoechst 33342. The *dashed* and *solid lines* indicate fluorescence intensities of the cells with and without dithionite treatment, respectively.

lation at the *sn*-1 position. We also synthesized lysoalkyl-EPA as a control (Fig. 1; see supplemental "Experimental Procedures" for the synthesis).

S. livingstonensis Ac10 was grown in the presence of lysoalkyl-EPA or methylalkyl-EPA, and the cellular phospholipids were analyzed by ESI-MS. The amounts of NBD-labeled phospholipids found incorporated into the cells were not significantly different between lysoalkyl-EPA and methylalkyl-EPA (Fig. 3). We also determined the amounts of NBD-labeled phospholipids distributed to the OM and IM by the dithionite quenching assay (Fig. 5). NBD-labeled phospholipids were found not only in the OM_{out} and OM_{in} + OM_{out}, but also in the IM_{in}, irrespective of whether lysoalkyl-EPA or methylalkyl-EPA was used. Thus, methylalkyl-EPA mimics lysoalkyl-EPA in these respects. On the other hand, methylalkyl-EPA is different from lysoalkyl-EPA in that methylalkyl-EPA was not acylated at the *sn*-1 position, as expected (Fig. 4). In the case of lysoalkyl-EPA, the *sn*-1 position was acylated, and the acyl chain composition at the *sn*-1 position was similar to that of the NBD-labeled phospholipids derived from acylalkyl-EPA (Table 1). Fluorescence microscopic analysis showed fluorescence localization at the center of the cells when lysoalkyl-EPA was added to the cells, whereas this localization was not observed when methylalkyl-EPA was used (Fig. 6). This finding suggested that the localization at the center of the cells was dependent on the acylation at the *sn*-1 position.

Fluorescence Microscopic Analysis of Cells Treated with Dithionite to Quench NBD Fluorescence in OM_{out}—S. livingstonensis Ac10 was grown at 6 °C for 250 h in the presence of acylalkyl-EPA or lysoalkyl-EPA, and the NBD fluorescence in the OM_{out} was quenched with sodium dithionite before fluorescence microscopic analysis as described under "Experimental Procedures" and supplemental "Experimental Procedures." The relative fluorescence intensity at the cell division site was increased by the dithionite treatment of both acylalkyl-EPA-labeled and lysoalkyl-EPA-labeled cells (Fig. 7).

DISCUSSION

Identity of Fluorescent Phospholipid Localized at Center of Cells during Cell Division—We found that the NBD-labeled fluorescent phospholipids localized to the nucleoid occlusion site at the cell center during cell division when acylalkyl-EPA was added to *S. livingstonensis* Ac10 (Figs. 2 and 6). This localization was eicosapentaenyl group-dependent because it was not observed when the cells were grown in the presence of acylalkyl-OLA. Notably, when another phospholipid containing the eicosapentaenyl group was used, namely dialkyl-EPA, this localization was not observed (Fig. 2). This may be because of the difference in their subcellular distribution. The NBD-labeled phospholipids were detected in the IM_{in} when acylalkyl-EPA was used, whereas the NBD-labeled phospholipids were not found in the IM_{in} with dialkyl-EPA (Fig. 5). This is

likely because the *sn*-1 position of dialkyl-EPA was not hydrolyzed, rendering it less capable of migrating into the IM_{in}. Because the OM_{in} and IM_{out} cannot be distinguished by the dithionite quenching assay, it is possible that the NBD-labeled phospholipids did not even reach the IM_{out} when dialkyl-EPA was used. Thus, the data indicate that the NBD-labeled phospholipids that localize at the nucleoid occlusion site may come from the IM. This view is supported by the fluorescence microscopic analysis of the cells treated with dithionite. Dithionite treatment of the cells to quench the NBD fluorescence at the OM_{out} increased relative fluorescence intensities at the cell division site (Fig. 7).

When we used diacyl-EPA, the cells were not labeled efficiently. This was probably due to the catalytic action of the OM phospholipase A (15, 26, 27); this enzyme likely catalyzed the cleavage of both ester-bonded hydrocarbon chains in diacyl-EPA. Thus, the resulting fluorescent *N*-NBD-*sn*-glycero-3-phosphoethanolamine was likely released from the OM because of its high hydrophilicity and was not subsequently incorporated into any cellular membrane components, rendering it impossible for us to detect it by fluorescence methods.

Acylalkyl-EPA was converted into lysoalkyl-EPA (Fig. 4, *white bars*) and then re-acylated to form NBD-labeled phospholipids with two hydrocarbon chains, one of which was the eicosapentaenyl group and the other an acyl group produced by the bacterial cells (Fig. 4, *black bars*). Thus, the fluorescent phospholipids observed in our study that localized to the cell center could be acylalkyl-EPA, lysoalkyl-EPA, or re-acylated phospholipids. We found that the fluorescent phospholipids localized to the center of the cells when lysoalkyl-EPA (but not methylalkyl-EPA) was used (Fig. 6). Methylalkyl-EPA mimics lysoalkyl-EPA in its distribution in the OM and IM but differs from lysoalkyl-EPA in that it cannot be acylated at the *sn*-1 position. Thus, the results suggest that the fluorescence localization at the nucleoid occlusion site was not due to lysoalkyl-EPA itself but was due to re-acylated phospholipids. In Gram-negative bacteria, 2-acylglycerophosphoethanolamine acyltransferase, an enzyme that catalyzes the acylation of lysophospholipids at the *sn*-1 position, is localized to the IM (28, 29). Considering that the NBD-labeled phospholipids were found in the IM when lysoalkyl-EPA was added to the cells (Fig. 5), acylation of lysoalkyl-EPA at the *sn*-1 position may have been catalyzed by this enzyme once it reached the IM; this allowed it to travel to the nucleoid occlusion site in the center of the bacterial cells.

Dialkyl-EPA and dialkyl-OLA did not reach the IM_{in} (Fig. 5), suggesting that phospholipids containing two hydrocarbon chains cannot traverse through the periplasmic space unless at least one of their hydrocarbon chains is cleaved off. The acyl group at the *sn*-1 position of acylalkyl-EPA and acylalkyl-OLA was probably hydrolyzed before they traversed through the periplasm to reach the IM. OM-resident phospholipase A most likely catalyzed this reaction to produce lysoalkyl-EPA and lysoalkyl-OLA, respectively (15, 26, 27). We suggest that lysoalkyl-EPA, produced by hydrolysis of acylalkyl-EPA, is re-acylated at its *sn*-1 position after reaching the IM, and the re-acylated NBD-labeled phospholipids are localized at the nucleoid occlusion site at the cell center during cell division.

Mechanisms and Significance of Formation of Membrane Microdomain Enriched in Polyunsaturated Hydrocarbon Chain-containing Phospholipids—We found that phospholipids containing an eicosapentaenyl group are enriched at the site of cell division. This is in accordance with our finding that EPA-containing phospholipids play an important functional role in the cell division in *S. livingstonensis* Ac10 (13). Although the molecular mechanism for the formation of the membrane domain enriched in polyunsaturated hydrocarbon chains remains unknown, we suggest the following two possibilities. The first is that the phospholipids containing the eicosapentaenyl group are enriched in a membrane region with a high curvature because of their physicochemical properties. We consider this possibility because the bending rigidity of bilayers rich in phospholipids with a polyunsaturated hydrocarbon chain is known to be low (30). The cellular membrane at the site of cell division has a high curvature, which may cause the enrichment of phospholipids with the eicosapentaenyl group in this region. The second possibility is that phospholipids containing an eicosapentaenyl group interact with proteins localized at the center of the cells during cell division. Considering that EPA-containing phospholipids promote cell division, there may be a direct or indirect interaction between these phospholipids and cell division-related proteins at the cell center. These interactions may cause enrichment of the eicosapentaenyl group-containing phospholipids at the site of cell division.

Polyunsaturated hydrocarbon chains have much greater diversity of energetically accessible conformational states than saturated hydrocarbon chains (31). This allows polyunsaturated hydrocarbon chains to solvate membrane proteins with rough surfaces with little energetic penalty. Thus, interaction with EPA-containing phospholipids may be beneficial for the stability and function of various membrane proteins, including those involved in cell division. The molecular interactions between EPA-containing phospholipids and membrane proteins involved in cell division are currently under investigation to better understand the role of EPA-containing phospholipids at the site of cell division. The occurrence of such membrane microdomains in other organisms and their specific physiological roles should also be examined in future studies. In this study, the visualization of the membrane microdomain enriched in phospholipids with a polyunsaturated hydrocarbon chain was made possible using a newly synthesized fluorescent probe with an uncleavable bond between the hydrocarbon chain and the glycerol backbone. This type of probe would be useful in examining whether membrane microdomains like the ones we observed in this study occur more generally among various organisms.

REFERENCES

1. Singer, S. J., and Nicolson, G. L. (1972) The fluid mosaic model of the structure of cell membranes. *Science* **175,** 720 –731
2. Lingwood, D., and Simons, K. (2010) Lipid rafts as a membrane-organizing principle. *Science* **327,** 46 –50
3. Matsumoto, K., Kusaka, J., Nishibori, A., and Hara, H. (2006) Lipid do-

mains in bacterial membranes. *Mol. Microbiol.* **61,** 1110–1117

4. Renner, L. D., and Weibel, D. B. (2011) Cardiolipin microdomains localize to negatively curved regions of *Escherichia coli* membranes. *Proc. Natl. Acad. Sci. U.S.A.* **108,** 6264–6269

5. López, D., and Kolter, R. (2010) Functional microdomains in bacterial membranes. *Genes Dev.* **24,** 1893–1902

6. Wall, R., Ross, R. P., Fitzgerald, G. F., and Stanton, C. (2010) Fatty acids from fish: the anti-inflammatory potential of long-chain ω-3 fatty acids. *Nutr. Rev.* **68,** 280–289

7. Watts, G. F., and Mori, T. A. (2011) Recent advances in understanding the role and use of marine ω-3 polyunsaturated fatty acids in cardiovascular protection. *Curr. Opin. Lipidol.* **22,** 70–71

8. Sato, S. B., Sato, S., Kawamoto, J., and Kurihara, T. (2011) Differential roles of internal and terminal double bonds in docosahexaenoic acid: comparative study of cytotoxicity of polyunsaturated fatty acids to HT-29 human colorectal tumor cell line. *Prostaglandins Leukot. Essent. Fatty Acids* **84,** 31–37

9. Schmitz, G., and Ecker, J. (2008) The opposing effects of *n*-3 and *n*-6 fatty acids. *Prog. Lipid Res.* **47,** 147–155

10. Feller, S. E., and Gawrisch, K. (2005) Properties of docosahexaenoic acid-containing lipids and their influence on the function of rhodopsin. *Curr. Opin. Struct. Biol.* **15,** 416–422

11. Carrillo-Tripp, M., and Feller, S. E. (2005) Evidence for a mechanism by which ω-3 polyunsaturated lipids may affect membrane protein function. *Biochemistry* **44,** 10164–10169

12. Grossfield, A., Feller, S. E., and Pitman, M. C. (2006) A role for direct interactions in the modulation of rhodopsin by ω-3 polyunsaturated lipids. *Proc. Natl. Acad. Sci. U.S.A.* **103,** 4888–4893

13. Kawamoto, J., Kurihara, T., Yamamoto, K., Nagayasu, M., Tani, Y., Mihara, H., Hosokawa, M., Baba, T., Sato, S. B., and Esaki, N. (2009) Eicosapentaenoic acid plays a beneficial role in membrane organization and cell division of a cold-adapted bacterium, *Shewanella livingstonensis* Ac10. *J. Bacteriol.* **191,** 632–640

14. Kawamoto, J., Sato, T., Nakasone, K., Kato, C., Mihara, H., Esaki, N., and Kurihara, T. (2011) Favorable effects of eicosapentaenoic acid on the late step of the cell division in a piezophilic bacterium, *Shewanella violacea* DSS12, at high hydrostatic pressures. *Environ. Microbiol.* **13,** 2293–2298

15. Sato, S., Kurihara, T., Kawamoto, J., Hosokawa, M., Sato, S. B., and Esaki, N. (2008) Cold adaptation of eicosapentaenoic acid-less mutant of *Shewanella livingstonensis* Ac10 involving uptake and remodeling of synthetic phospholipids containing various polyunsaturated fatty acids. *Extremophiles* **12,** 753–761

16. Kawamoto, J., Kurihara, T., Kitagawa, M., Kato, I., and Esaki, N. (2007) Proteomic studies of an Antarctic cold-adapted bacterium, *Shewanella livingstonensis* Ac10, for global identification of cold-inducible proteins. *Extremophiles* **11,** 819–826

17. Miyake, R., Kawamoto, J., Wei, Y. L., Kitagawa, M., Kato, I., Kurihara, T., and Esaki, N. (2007) Construction of a low temperature protein expression system using a cold-adapted bacterium, *Shewanella* sp. strain Ac10, as the host. *Appl. Environ. Microbiol.* **73,** 4849–4856

18. Reutelingsperger, C. P., Dumont, E., Thimister, P. W., van Genderen, H., Kenis, H., van de Eijnde, S., Heidendal, G., and Hofstra, L. (2002) Visualization of cell death *in vivo* with the annexin A5 imaging protocol. *J. Immunol. Methods* **265,** 123–132

19. Emoto, K., and Umeda, M. (2000) An essential role for a membrane lipid in cytokinesis. Regulation of contractile ring disassembly by redistribution of phosphatidylethanolamine. *J. Cell Biol.* **149,** 1215–1224

20. Jao, C. Y., Roth, M., Welti, R., and Salic, A. (2009) Metabolic labeling and direct imaging of choline phospholipids *in vivo*. *Proc. Natl. Acad. Sci. U.S.A.* **106,** 15332–15337

21. Kuerschner, L., Ejsing, C. S., Ekroos, K., Shevchenko, A., Anderson, K. I., and Thiele, C. (2005) Polyene lipids: a new tool to image lipids. *Nat. Methods* **2,** 39–45

22. Neef, A. B., and Schultz, C. (2009) Selective fluorescence labeling of lipids in living cells. *Angew. Chem. Int. Ed. Engl.* **48,** 1498–1500

23. Yamaji, A., Sekizawa, Y., Emoto, K., Sakuraba, H., Inoue, K., Kobayashi, H., and Umeda, M. (1998) Lysenin, a novel sphingomyelin-specific binding protein. *J. Biol. Chem.* **273,** 5300–5306

24. Bligh, E. G., and Dyer, W. J. (1959) A rapid method of total lipid extraction and purification. *Can. J. Biochem. Physiol.* **37,** 911–917

25. Shindou, H., Hishikawa, D., Harayama, T., Yuki, K., and Shimizu, T. (2009) Recent progress on acyl-CoA:lysophospholipid acyltransferase research. *J. Lipid Res.* **50,** S46–S51

26. Malinverni, J. C., and Silhavy, T. J. (2009) An ABC transport system that maintains lipid asymmetry in the Gram-negative outer membrane. *Proc. Natl. Acad. Sci. U.S.A.* **106,** 8009–8014

27. Dekker, N. (2000) Outer membrane phospholipase A: known structure, unknown biological function. *Mol. Microbiol.* **35,** 711–717

28. Harvat, E. M., Zhang, Y. M., Tran, C. V., Zhang, Z., Frank, M. W., Rock, C. O., and Saier, M. H., Jr. (2005) Lysophospholipid flipping across the *Escherichia coli* inner membrane catalyzed by a transporter (LplT) belonging to the major facilitator superfamily. *J. Biol. Chem.* **280,** 12028–12034

29. Hsu, L., Jackowski, S., and Rock, C. O. (1991) Isolation and characterization of *Escherichia coli* K-12 mutants lacking both 2-acylglycerophosphoethanolamine acyltransferase and acyl-acyl carrier protein synthetase activity. *J. Biol. Chem.* **266,** 13783–13788

30. Rawicz, W., Olbrich, K. C., McIntosh, T., Needham, D., and Evans, E. (2000) Effect of chain length and unsaturation on elasticity of lipid bilayers. *Biophys. J.* **79,** 328–339

31. Feller, S. E. (2008) Acyl chain conformations in phospholipid bilayers: a comparative study of docosahexaenoic acid and saturated fatty acids. *Chem. Phys. Lipids* **153,** 76–80

32. Mileykovskaya, E., and Dowhan, W. (2009) Cardiolipin membrane domains in prokaryotes and eukaryotes. *Biochim. Biophys. Acta* **1788,** 2084–2091